

See discussions, stats, and author profiles for this publication at: <https://www.researchgate.net/publication/275525386>

Comprehensive Study of Methylation on Silicon (100)-2 x 1 Surface: A Density Functional Approach

ARTICLE *in* THE JOURNAL OF PHYSICAL CHEMISTRY A · APRIL 2015

Impact Factor: 2.69 · DOI: 10.1021/acs.jpca.5b01148 · Source: PubMed

READS

29

5 AUTHORS, INCLUDING:



Kaushik Sen

University of Cambridge

19 PUBLICATIONS 32 CITATIONS

[SEE PROFILE](#)



Deepanwita Ghosh

Indian Association for the Cultivation of Science

26 PUBLICATIONS 43 CITATIONS

[SEE PROFILE](#)

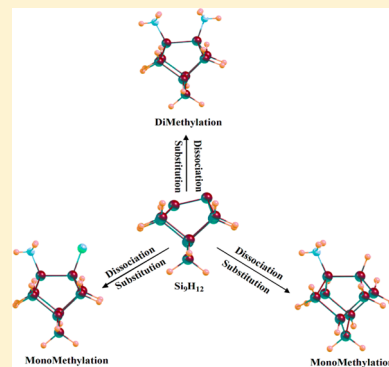
Comprehensive Study of Methylation on the Silicon (100)-2 × 1 Surface: A Density Functional Approach

Tanay Debnath, Kaushik Sen, Deepanwita Ghosh, Tahamida Banu, and Abhijit K. Das*

Department of Spectroscopy, Indian Association for the Cultivation of Science, Jadavpur, Kolkata 700032, India

S Supporting Information

ABSTRACT: A detailed mechanistic investigation of Si–Me formation over the silicon (100)-2 × 1 surface using the Si_9H_{12} cluster model has been performed using various reagents, based on two basic mechanisms: dissociation and substitution. The reagents CH_4 , CH_3Cl for dissociation and CH_3Li , CH_3MgBr for substitution mechanism are used to explore the methylation process on the silicon surface at the M062X/6-311+G(2d, p) level of theory. The associated potential energy surfaces explored here are aimed to unveil the most favored pathway of methylation with appropriate reagents. Dissociation of methane forms a monomethylated product (D1) through an energetically unfavorable pathway. All the adsorption modes of CH_3Cl over the silicon surface are also detected and analyzed. Methyl chloride dissociates to form another monomethylated product D2 and its derivative D3 in the entrance channel, while, in the next step, bridged compounds I1 (Cl-bridged) and I2 (H-bridged) are produced from them, respectively. The C–Cl dissociation leads to the formation of D2 having a lower activation barrier. With a comparably high activation barrier in the C–H dissociation, producing D3, very interestingly carbene intermediate has been detected in the reaction pathway. Detection of energetically unfavored conversions from D2 to I1 and D3 to I2 ensured that the methylation process will not be hampered through these interconversions. For substitution, HCl- and Cl_2 -passivated Si surfaces are taken, where chlorine is to be substituted by the methyl group of both of the methylating agents. With both substituents, HCl-passivated Si_9H_{12} gives D1. The substitution process on Cl_2 -passivated Si_9H_{12} leads to the formation of D2 in the first step and dimethylated product (S1) in the final step. In all the above substitution processes, methyl lithium proved to be the better substituent for the formations of D1, D2, and S1 on HCl- or Cl_2 -passivated surfaces. The present work not only demonstrated methyl lithium as one of the best methylating agents but also revealed the interrelation among the dissociative adsorption modes of CH_3Cl , reported earlier, in a single potential energy surface with a remarkable detection of carbene intermediate formed in the pathway of C–H dissociation.



INTRODUCTION

It is well-known that the clean Si (100)-2 × 1 surface provides remarkable templates for the covalent attachment of various compounds fulfilling the purpose of generating different types of hybrid devices.^{1–12} Formation of a silicon–carbon bond on the silicon surface as well as on porous silicon has received considerable attention in this context in recent decades and is established to give rise to a promising class of materials. Consequently, the growth of the silicon carbide thin film on the silicon surface has emerged as an important area of research. Silicon carbide thin films span applications from microelectronics^{12–14} to nanotechnology. Formation of a Si–C bond on a silicon surface is also found to be a viable technique for surface termination, as the Si–C bond is inert, unpolarized, and less susceptible toward nucleophilic substitution^{15–17} than Si–Cl and also Si–H and thus it can protect the surface from air oxidation and give kinetic inertness. Thus, Si–C covalent linkage can be utilized in passivating different types of Si–C–R mono layer over the silicon surface, where R is any organic groups or biological fragments. Different routes like chemical,¹⁸ thermochemical,¹⁹ photochemical,²⁰ and electrochemical²¹ processes are adopted for depositing compounds over the

silicon surface. The formation of the desired Si–C bond can be achieved through passivation of the silicon surface via several processes using alkyl halide,^{22,23} alkyl silane,²⁴ Grignard reagents,^{25–27} alkyl lithium,²⁸ alkanes,^{29,30} alkenes,³¹ alkynes,³² etc., where carbon contains hydrogen only. Among various alkyl groups, the methyl–silicon linkage on the silicon surface is interesting, as it has some unique characters different from others. It is observed that the methyl group has an advantage to fit on the silicon surface, as it is the smallest among the alkyl groups and it also forms a stable and strong covalent bond compared to other alkyl groups as well as halides and hydrides. Lee et al.²² have observed the adsorption modes and dissociation process of methyl halide on the Si (100)-2 × 1 surface, leading to the formation of a Si–Me bond. They have investigated the adsorption and dissociation mechanism of CH_3Cl on the Si (100)-2 × 1 surface using AES and LEED and also the semiempirical (PM3) method. Romero et al.²³ have modified and extended the work and checked the adsorption

Received: February 4, 2015

Revised: April 27, 2015

Published: April 27, 2015

modes employing different ab initio and density functional based methods. They have investigated the pathway of dissociation of CH_3Cl over the silicon surface through different transition state search processes using slab geometry and also with STM images. A number of works have been carried out on the formation of Si–C bonds by Grignard reagents and alkyl lithium on porous silicon and also on a silicon surface. Vegunta et al.²⁶ have worked on passivating the Si (100) surface with methyl and ethyl groups using a Grignard reagent through electrochemical and thermal grafting processes. Electrochemical grafting has been performed using a hydride terminated surface, while a chloride terminated surface is used for thermal grafting. Amy et al.²⁵ have also investigated the alkylation process on a Cl_2 terminated Si (111) surface. They have analyzed the two-step gas phase reaction that takes place during alkylation, chlorination followed by alkylation through Grignard reagent. Song and Sailor have proposed generation of a Si–C bond on porous silicon using aryl lithium.²⁸

In spite of implementation of several mechanisms of methylation on the silicon surface with several substrates, no one has paid attention to promoting the most promising mechanistic process with appropriate reagents. In the present work, we have aimed at investigating the best way of methylation using comparative theoretical analysis among two basic mechanisms, i.e., dissociation of methane and methyl chloride and substitution with methyl lithium and Grignard reagent on HCl- and Cl_2 -passivated surfaces exploring all the associated potential energy surfaces. To model the silicon (100)-2 × 1 surface, we have used a Si_9H_{12} cluster where the upper silicon dimer has been represented as a surface. In our work, a two-atom-modeled surface is sufficient, as there is no dative bond beyond the two atom surface space in the adsorption process and in reaction mechanisms and, second, all the reactions adopted here are involved in either one bond dissociation or a one to one substitution process on the silicon surface. The cluster^{33–48} has also been proved to be best represented as a single dimer cluster for observing the surface mechanisms especially adsorption and dissociation processes and gave satisfactory results comparable with the experimental values for small molecules like CO ,³⁴ HCN ,³⁵ Lewis acids,³⁷ alcohols,^{36,46} amines,⁴⁶ cyclic systems,⁴⁰ organosulfurs,⁴¹ metal oxide,⁴³ amino acids,⁴⁷ etc. Very recently, Raghavachari et al.⁴⁸ have also used the cluster to observe the hydrogen abstraction mechanism on the silicon surface. Raghavachari et al.⁴⁵ have also reported a substitution process on water-passivated Si_9H_{12} with Al_2O_3 . Therefore, it is justified to take a Si_9H_{12} single dimer cluster as a template for the silicon (100)-2 × 1 surface to observe mainly C–Cl or C–H dissociations and Si–Cl to Si–C substitution processes.

Following is a schematic presentation of the fundamental processes investigated here for Si–Me bond formation with varying reagents.

While Schemes 1 and 2 indicate the dissociation processes, Schemes 3 and 4 refer to the substitution processes. As shown in Scheme 1, we have taken the simple methane molecule to

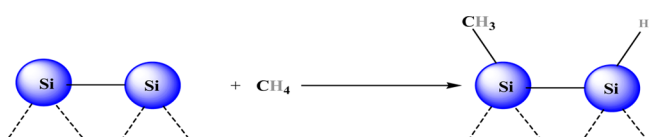
study its dissociation to form a Si–Me bond on the silicon surface, though this process is expected to be less favored as the C–H bond is too strong to dissociate with the small difference in polarity between carbon and hydrogen. Considering the dissociation of methyl chloride depicted in Scheme 2, we have thoroughly reinvestigated the methyl halide adsorption modes prior to dissociation. Our calculation unveiled some new outcomes related to adsorption phenomena which were not reported in the earlier investigations by Lee et al. and Romero et al. The most stable adsorption mode is taken as a starting reactant in Scheme 2 where CH_3Cl dissociates to either Si– CH_3 or Si– CH_2Cl and further interconverted in bridged compounds, resulting in 50% surface coverage of methylation in the entrance channel.

Though a number of experimental investigations have been carried out on the much imperative passivation of porous silicon or silicon surface by methyl group employing methyl lithium and Grignard reagent, no theoretical attempt has been made in this regard, to the best of our knowledge. In the present theoretical study, we have thoroughly investigated the methyl passivation mechanism using methyl lithium and Grignard reagent by considering the HCl and Cl_2 terminated surface in Schemes 3 and 4. In Scheme 3, we have used the HCl terminated surface where both the reagents substitute surface chlorine by a methyl group, indicating surface silicones are alternatively methylated, leading to 50% surface coverage. In Scheme 4, a double chloride (Cl_2) terminated surface is considered for methyl passivation using the same reagents where both chlorines are substituted by a methyl group, rendering continuous methylation of all surface silicones, yielding 100% surface coverage. Considering the ease of substitution, as already known, the Si–C bond is more stable than Si–Cl on the silicon surface and also magnesium and lithium possess a high affinity for chlorine, causing easy substitution of surface chlorine by a methyl group. It should be noted here that hydrogen can also be substituted by a methyl group of Grignard reagent electrochemically which follows a completely radical like mechanism, and thus, it is difficult to detect any substitution mechanism in a concerted $S_{\text{N}2}$ like thermal process.

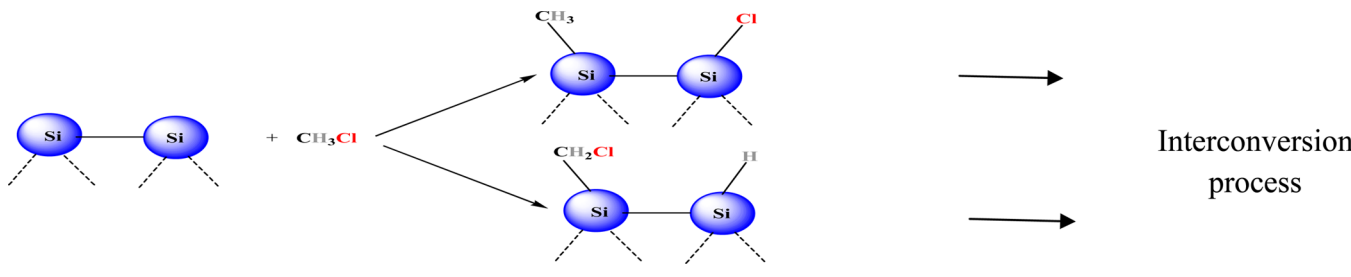
COMPUTATIONAL DETAILS

In exploring potential energy surfaces, the participating reactants, transition states, and products associated with the dissociation and substitution processes are optimized using the hybrid functional M062X along with the basis set 6-311+G-(2d,p) for all the atoms without any geometry and symmetry constraints, as no unphysical distortions of the surface model were witnessed.⁴⁹ The thorough examination of the optimized structures showed no significant changes in cluster geometries. The M062X (from M06 family) developed by Truhlar and Zhao⁵⁰ is well recommended for applications involving main group thermochemistry, noncovalent interaction, etc. The superiority of the contemporary M06 family in studying reactions on Si_9H_{12} cluster is also established by the recent work of Raghavachari et al.⁴⁸ The harmonic vibrations of all the optimized geometries are analyzed at the same level to reveal the nature of the stationary points. The minima (local and global) on the PESs are identified by the presence of all real frequencies, whereas each transition state structure is characterized by one imaginary frequency. The intrinsic reaction coordinate (IRC)^{51,52} calculations are carried out to trace the reaction paths from the transition states in mass-

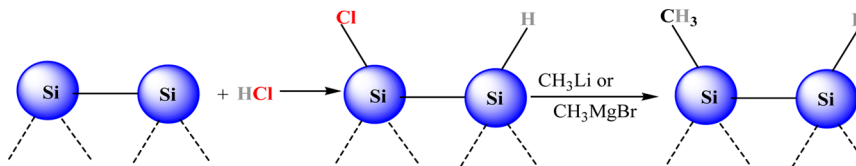
Scheme 1



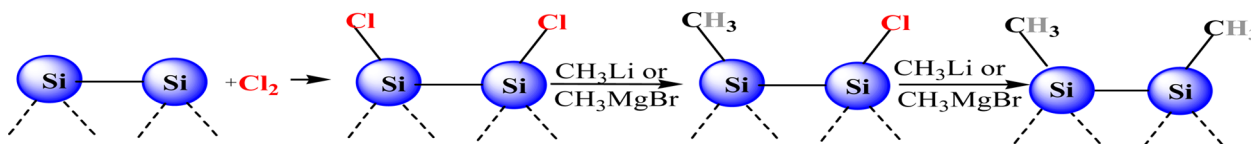
Scheme 2



Scheme 3



Scheme 4



weighted internal coordinate (S_b), going in forward and reverse directions. This confirms the connection between a particular transition state with specific reactant and product. To accurately calculate the adsorption energies for various modes of CH_3Cl over the silicon surface, Grimme's D3^{53,54} dispersion correction and basis set superposition error (BSSE) correction are considered. BSSE correction is determined through counterpoise correction.^{55,56} Though the M06 suite of functionals already takes dispersion into account, Goerigk and Grimme⁵⁷ have demonstrated that the addition of D3 corrections improves the performance of the Minnesota class of functional. For this reason, we have estimated Grimme's D3 dispersion correction with optimized geometry of physisorption modes to incorporate the fine refinement. All of these above calculations are performed using the Gaussian 09⁵⁸ program. To visualize atom to atom interaction and to analyze bond critical points in the adsorption modes of CH_3Cl on Si_9H_{12} as well as bonding evolution, we have used AIM all⁵⁹ in our present work. The AIM theory developed by Bader⁶⁰ is a powerful method to analyze the molecular structures, making a link between quantum mechanics and standard chemical concepts for the study of bonding using only the charge density distribution $\rho(r)$. We can identify critical points in the charge density distribution where $\nabla\rho(r) = 0$, and further classify these points according to the properties of the three eigenvalues λ_1 , λ_2 , and λ_3 ($\lambda_1 < \lambda_2 < \lambda_3$) of the diagonalized Hessian of $\rho(r)$.

RESULTS AND DISCUSSION

In the present section, the outcomes of the investigation of Si-Me formation over the silicon (100)-2 × 1 surface (Si_9H_{12} cluster model) through dissociation and substitution mechanisms using various reagents are discussed. Our calculations have revealed that the Si (100)-2 × 1 surface dimer is buckled or tilted. This tilting renders the dimer a zwitterion-like

character in which the "down" silicon atom is slightly positive relative to the "up" silicon atom. The up silicon is comparatively electron rich as compared with the down silicon. Here this buckling effect is an essential feature for adsorption and dissociation processes. In studying the methylation processes, the potential energy surfaces (PES) have been constructed at the M06-2X/6-311+G (2d,p) level of theory. All the physisorption modes are shown in Figure 1, and all the dissociative adsorption modes including all the methylated products form in dissociation and substitution process are shown in Figure 2. The reactants and transition states of all dissociation and substitution processes are shown in Figure 3. The potential energy surfaces are shown in Figures 4–10. All the significant data associated with our results are depicted in Tables 1–3. All the energy values are reported in 0 °C.

Dissociation Process. The complete potential energy surface, activation barrier, and reaction enthalpies for the dissociation processes are explored and reported herein at the M06-2X/6-311+G (2d,p) level of theory. Two types of plausible dissociation processes are investigated over the silicon surface: (i) dissociation of methane to form D1 (shown in Figure 2) and (ii) dissociation of CH_3Cl to get four types of dissociative adsorption modes, D2, D3, I1, and I2 (shown in Figure 2), respectively. The details of the two dissociation processes are outlined below.

Methylation through Dissociation of CH_4 . Dissociation of methane on the silicon surface produces D1 where the Si-Me bond is formed between alternate silicon atoms on the surface. The corresponding potential energy surface, PES1, is depicted in Figure 4. The dissociation process is found to pass through a well-defined transition state with a very high activation barrier of 48.53 kcal/mol. Thus, the dissociation process is clearly kinetically disfavored. This can be attributed to the chemical inertness of the C-H bond. However, noticeably, the dissociation process is associated with a high exothermicity of 46.87 kcal/mol, indicating that this type of

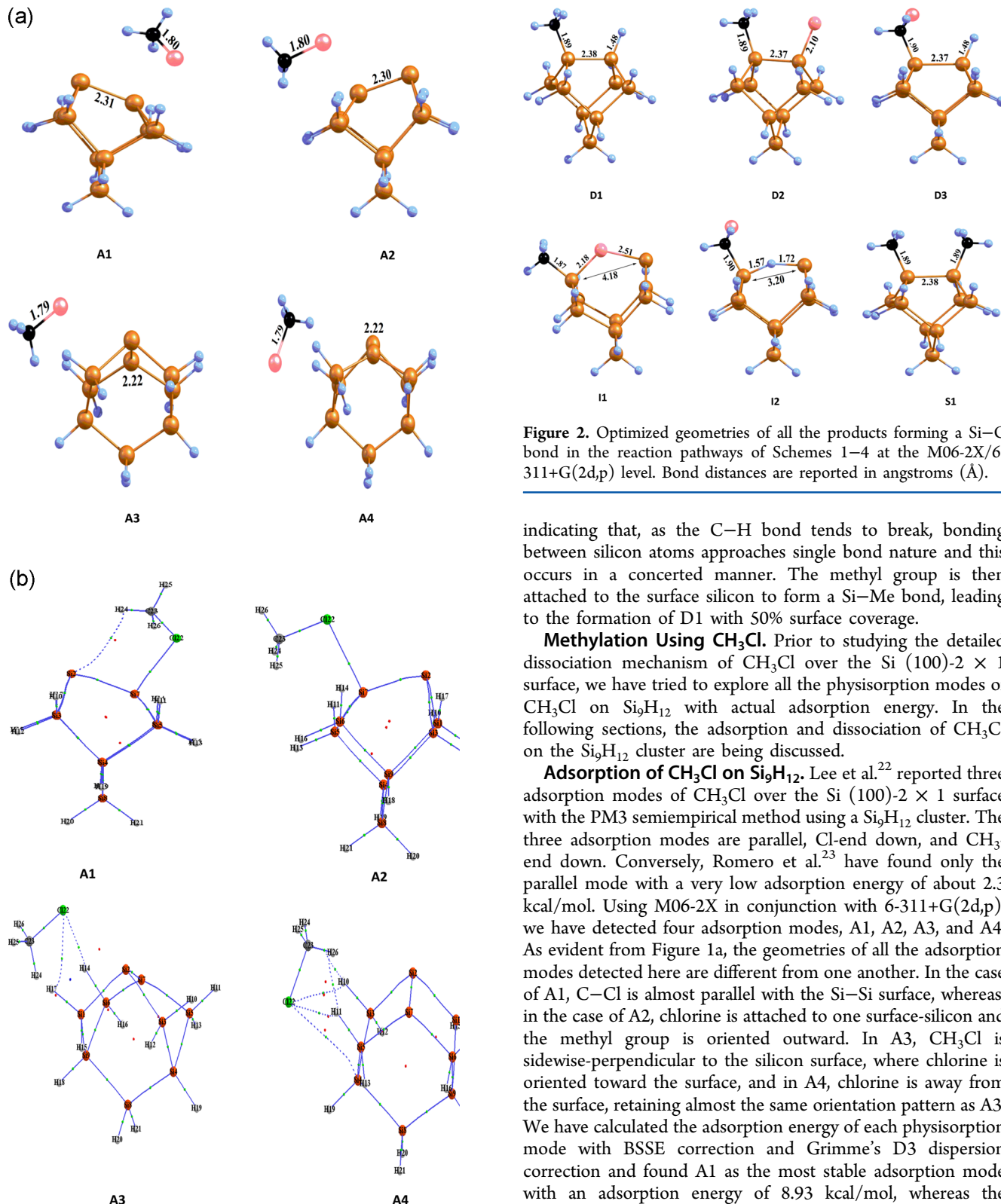


Figure 1. (a) Different physisorption geometries of CH_3Cl over Si_9H_{12} cluster at the M06-2X/6-311+G(2d,p) level. Bond distances are reported in angstroms (\AA). (b) Charge density topology of geometries of part a.

methylation process is thermodynamically favored. An inspection of the geometry of the transition state reveals that both Si–Si and C–H bonds become elongated at $\text{TS}_{\text{d}1}$,

Figure 2. Optimized geometries of all the products forming a Si–C bond in the reaction pathways of Schemes 1–4 at the M06-2X/6-311+G(2d,p) level. Bond distances are reported in angstroms (\AA).

indicating that, as the C–H bond tends to break, bonding between silicon atoms approaches single bond nature and this occurs in a concerted manner. The methyl group is then attached to the surface silicon to form a Si–Me bond, leading to the formation of D1 with 50% surface coverage.

Methylation Using CH_3Cl . Prior to studying the detailed dissociation mechanism of CH_3Cl over the Si (100)-2 \times 1 surface, we have tried to explore all the physisorption modes of CH_3Cl on Si_9H_{12} with actual adsorption energy. In the following sections, the adsorption and dissociation of CH_3Cl on the Si_9H_{12} cluster are being discussed.

Adsorption of CH_3Cl on Si_9H_{12} . Lee et al.²² reported three adsorption modes of CH_3Cl over the Si (100)-2 \times 1 surface with the PM3 semiempirical method using a Si_9H_{12} cluster. The three adsorption modes are parallel, Cl-end down, and CH_3 -end down. Conversely, Romero et al.²³ have found only the parallel mode with a very low adsorption energy of about 2.3 kcal/mol. Using M06-2X in conjunction with 6-311+G(2d,p), we have detected four adsorption modes, A1, A2, A3, and A4. As evident from Figure 1a, the geometries of all the adsorption modes detected here are different from one another. In the case of A1, C–Cl is almost parallel with the Si–Si surface, whereas, in the case of A2, chlorine is attached to one surface-silicon and the methyl group is oriented outward. In A3, CH_3Cl is sideways-perpendicular to the silicon surface, where chlorine is oriented toward the surface, and in A4, chlorine is away from the surface, retaining almost the same orientation pattern as A3. We have calculated the adsorption energy of each physisorption mode with BSSE correction and Grimme's D3 dispersion correction and found A1 as the most stable adsorption mode with an adsorption energy of 8.93 kcal/mol, whereas the adsorption energy of A2 is 8.08 kcal/mol followed by 3.89 kcal/mol for A3 and 3.38 kcal/mol for A4.

The adsorption of CH_3Cl over the silicon surface brings about no significant changes to the geometry of the whole system, leaving the adsorbate intact and the surface unmolested. However, the effect of adsorption is clearly reflected in the change of bond distance between surface silicon atoms. In the bare cluster, the Si–Si bond length is almost double bond like character as the Si–Si single bond length is known to be 2.33 \AA .

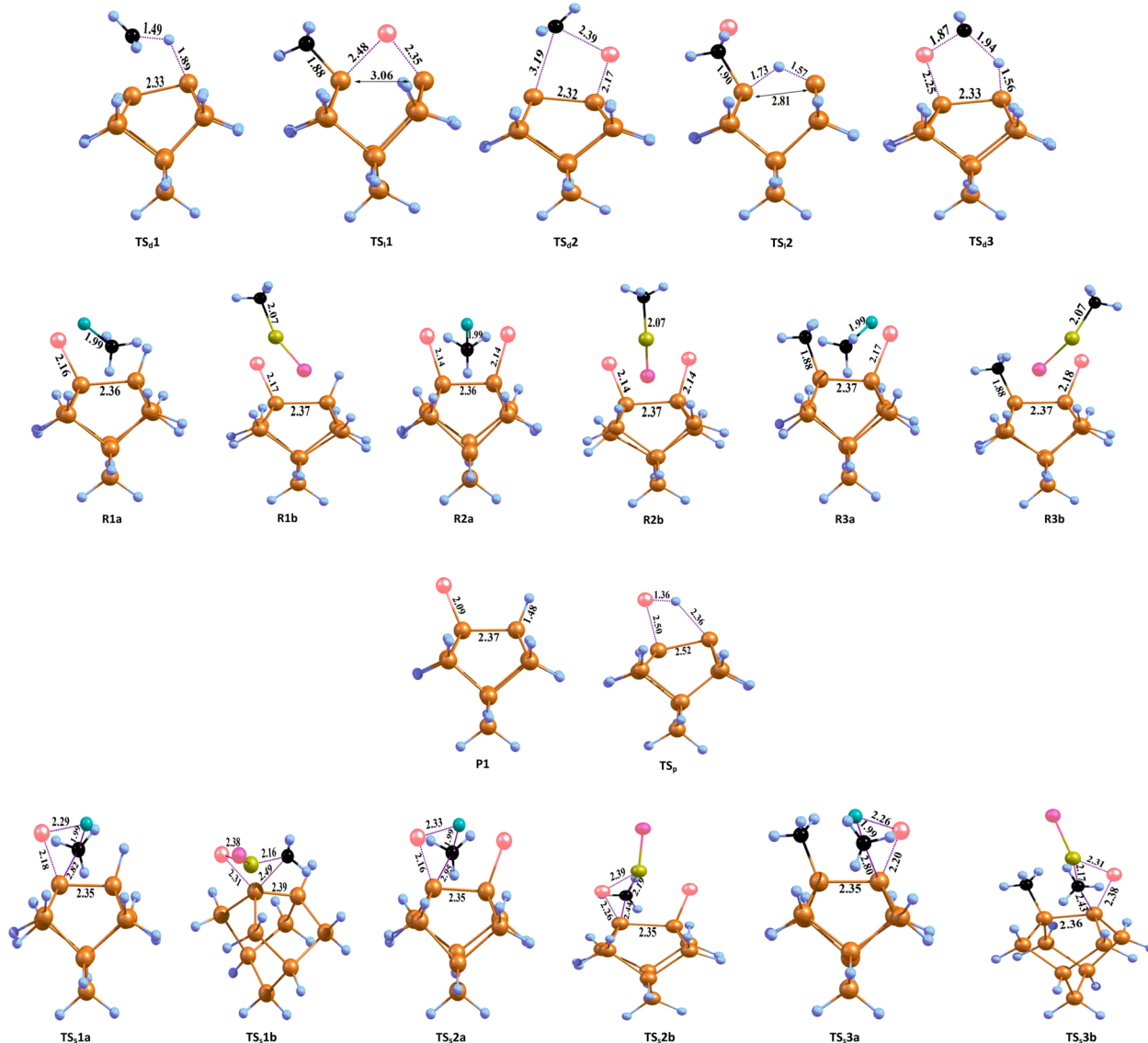


Figure 3. Optimized geometries of adducts and TSs occurring in the reaction pathways of Schemes 1–4 at the M06-2X/6-311+G(2d,p) level. Bond distances are reported in angstroms (\AA).

Table 1. Adsorption Energy (in kcal/mol) of Four Adsorption Modes of CH_3Cl on the Si_9H_{12} (100) 2×1 Surface at the M06-2X/6-311+G(2d,p) Level with Grimme's D3 Dispersion Correction and Basis Set Superposition Error Correction

adsorption mode	adsorption energy
A1	8.93
A2	8.08
A3	3.89
A4	3.38

In A1, the bond length increases to 2.31 Å and the corresponding binding energy is calculated to be 8.93 kcal/mol. However, the change in the bond length of C–Cl in CH_3Cl in the adsorbed state is negligibly small and this is valid for all the physisorption modes. A noticeable change in the bond length of Si–Si is also observed for A2, while for A3 and A4 the Si–Si bond length remains unaltered. All the Si–Si and C–Cl bond lengths of all four adsorption modes are depicted in Figure 1a. To get better insight into the adsorption modes

and interaction between adsorbate and surface silicon dimer, AIM analysis is also employed, as shown in Figure 1b. The most tightly bound A1 mode exhibits complete surface adhesion through $\text{Si}7\text{–Cl}22$ and $\text{Si}2\text{–H}24$ interactions, where $\text{Si}2\text{–Si}7$ is considered as a surface dimer in the Si_9H_{12} single dimer cluster. The next significant surface adsorption mode is realized in conformer A2. Here, surface adhesion is characterized by the $\text{Si}7\text{–Cl}22$ interaction only. It is interesting to note that the characteristics of the Si–Cl BCPs like charge density $\rho(r_c)$, Laplacian of charge density $\nabla^2\rho(r_c)$, and bond ellipticity ϵ in A1 and A2 (see Table 2) revealed that the Si–Cl interaction is stronger in the former. On the other hand, as supported by the AIM analysis, the atoms of the CH_3Cl molecule do not exhibit any interaction with the surface silicon dimer ($\text{Si}2\text{–Si}7$) in the case of A3 and A4 and, consequently, there is no change of the bond length of the surface silicon dimer. Hence, it can be concluded that A3 and A4 may be discarded as adsorption modes contrary to the acceptable A1 and A2 adsorption modes.

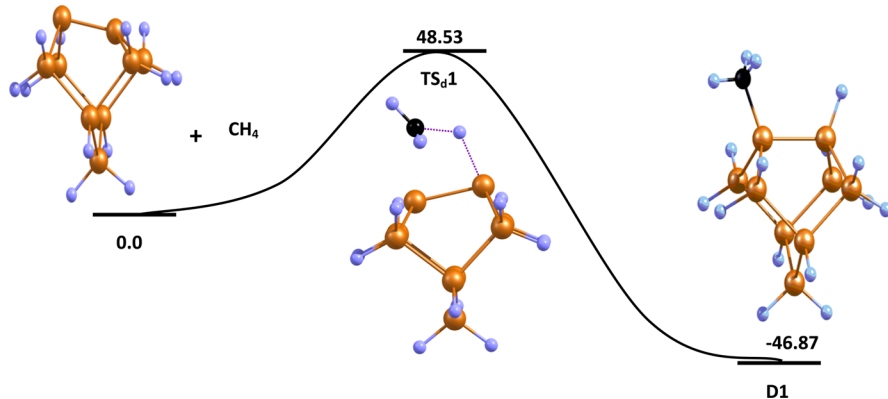


Figure 4. Potential energy surface for dissociation of CH_4 on Si_9H_{12} at the M06-2X/6-311+G(2d,p) level (PES1) in kcal/mol.

Table 2. Electronic Densities $\rho(r_c)$, Eigenvalues of Hessian Matrix ($\lambda_1, \lambda_2, \lambda_3$), Laplacian of Electron Densities ($\nabla^2\rho(r_c)$), and Bond Ellipticities (ϵ) at Critical Points of Associated Bonds in Physisorption Modes

species	bond	$\rho(r_c)$	λ_1	λ_2	λ_3	ϵ	$\nabla^2\rho(r_c)$
A1	Si7–Cl22	0.041	-0.024	-0.022	0.072	0.087	0.025
	Si2–H24	0.008	-0.005	-0.001	0.025	4.751	0.019
A2	Si7–Cl22	0.040	-0.022	-0.021	0.069	0.006	0.026

Dissociation of CH_3Cl . We have explored the full reaction profile corresponding to all possible dissociative adsorption modes for the dissociation of CH_3Cl over the silicon surface. In this connection, it should be mentioned here that Romero et al.²³ have identified four dissociative adsorption modes of CH_3Cl over the silicon surface. The four dissociative adsorption modes, D2, D3, I1, and I2, identified in this present study are displayed in Figure 2. The D2 mode is obtained through C–Cl bond dissociation where one surface silicon is attached with methyl and the other is bonded with chlorine and gives 50% surface coverage. Likewise, for D3, one silicon is attached to the CH_2Cl moiety and the other is bonded with hydrogen. Both dissociative adsorption modes are obtained through well-defined transition states and are a one-step process. The bridged modes, i.e., I1 and I2, cannot be directly obtained from physisorption modes. It is observed that D2 interconverts to I1 and D3 interconverts to I2. The complete potential energy surface, designated as PES2, is shown in Figure 5.

As evident from Figure 5, the process of C–Cl bond dissociation, leading to D2, passes through the transition state $\text{TS}_{\text{d}2}$ with a comparatively lower activation barrier than C–H bond dissociation, leading to D3. Formation of D2 is found to be associated with an activation barrier of 26.48 kcal/mol, whereas formation of D3 possesses an activation barrier of 36.23 kcal/mol and thus the former is kinetically favored over the latter. This also holds from a thermodynamic perspective, as the former is associated with an exothermicity of 77.38 kcal/mol, while the latter possesses an exothermicity of 40.06 kcal/mol. In the case of C–Cl bond dissociation, chlorine is found to be bonded with more positive down-silicon and methyl is attached to the electron rich up-silicon. It is apparent from the associated cyclic four-member transition state that chlorine almost forms a covalent bond with the silicon surface and the C–Cl bond distance becomes 2.42 Å (C–Cl single bond length 1.78 Å), indicating that the C–Cl bond is almost ruptured. The transition state vector shows that the methyl group has a tendency to go to the electron poor silicon atom on the surface. The C–H dissociation process is very interesting to observe. Analysis of the reaction pathway through IRC reveals that the

process passes through a carbene intermediate, but this cannot be located on the potential energy surface due to the very reactive nature of the species. Actually, it is generated in situ and further takes part in the insertion process. To reveal this mechanism, the bonding evolution along the IRC path from $\text{TS}_{\text{d}3}$ to the product D3 has been carried out through the AIM formalism which shows that the pathway goes through four distinct SSDs. As the reaction proceeds from the transition state $\text{TS}_{\text{d}3}$, the first SSD exhibits a RCP for the ring structure $\text{Si}_2\text{H}_{24}\text{C}_{23}\text{Cl}_{22}\text{Si}_7$. The $\text{C}_{23}\text{Cl}_{22}$ and $\text{C}_{23}\text{H}_{24}$ bonds get weaker as their separation increases with the progress of the reaction in the first SSD signifying the production of the in situ carbene intermediate. The failure of detection of the carbene intermediate may be attributed to the very unstable nature of $:\text{CH}_2$. The $\text{C}_{23}\text{H}_{24}$ hydrogen bond finally breaks, and consequently, the first SSD gets converted into the second SSD through bifurcation catastrophe. In the due course of reaction, both the bonds $\text{Si}_7\text{Cl}_{22}$ and $\text{C}_{23}\text{Cl}_{22}$ in the second SSD become weaker as the $\text{C}_{23}\text{H}_{25}\text{H}_{26}$ moiety approaches the silicon surface toward the Si_7 atom. The second SSD enters into the third SSD through bifurcation catastrophe as the BCP of Si_7C_{23} and the RCP of $\text{Si}_7\text{C}_{23}\text{Cl}_{22}$ appear almost overlapping on each other. While the reaction proceeds, the RCP of $\text{Si}_7\text{C}_{23}\text{Cl}_{22}$ moves from the BCP of Si_7C_{23} toward the BCP of $\text{Si}_7\text{Cl}_{22}$ as a consequence of the weakening of the silicon–chlorine interaction. Interestingly, in this time, the $\text{C}_{23}\text{Cl}_{22}$ separation decreases and the interaction increases, changing from weak electrovalent to covalent interaction. Hence, a carbene insertion mechanism is realized. The third SSD enters into the fourth SSD through another bifurcation catastrophe with disappearance of both the BCP of $\text{Si}_7\text{Cl}_{22}$ and the RCP of $\text{Si}_7\text{C}_{23}\text{Cl}_{22}$. In the fourth SSD, both the Si_7C_{23} and $\text{C}_{23}\text{Cl}_{22}$ covalent interactions increase as the reaction heads toward the product D3. We have shown significant charge density topology in each of the above SSDs for generation of carbene and its insertion process in Figure 6.

Both of the dissociation processes are subsequently followed by interconversion, where chlorine and hydrogen, bonded with

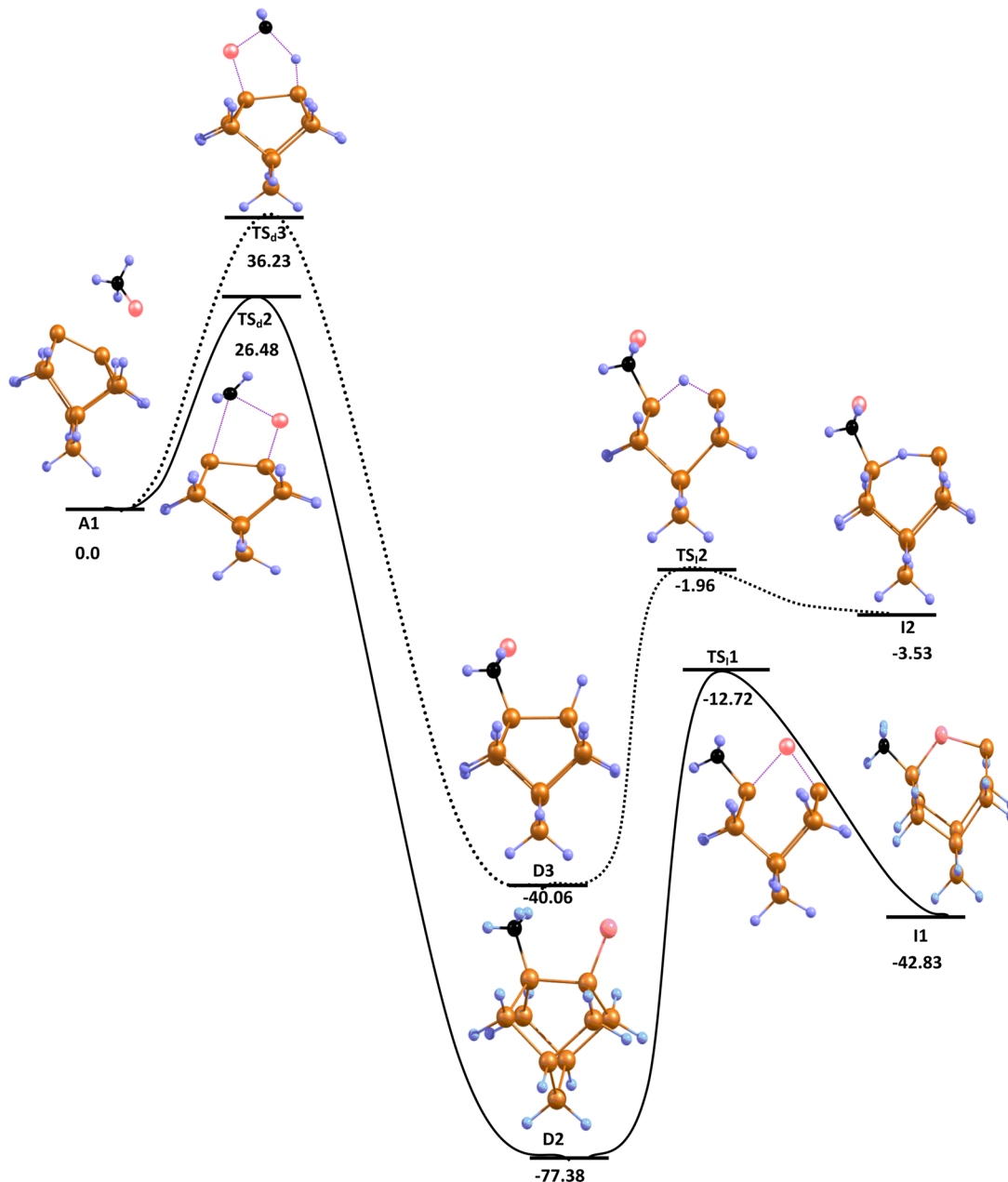


Figure 5. Potential energy surface for dissociation of CH_3Cl on Si_9H_{12} at the M06-2X/6-311+G(2d,p) level (PES2) in kcal/mol.

one surface silicon, attack the neighboring surface silicon attached with methyl and methyl halide groups, respectively, and this leads to the complete breakage of the Si–Si bond, resulting in the formation of I1 and I2, respectively. The I1 mode is obtained through the transition state $\text{TS}_{\text{I}1}$ with a very high activation barrier of 64.66 kcal/mol. The process is also found to be highly endothermic by 34.55 kcal/mol, indicating that this interconversion process is disfavored kinetically as well as thermodynamically. I2 is also obtained through a well-defined transition state $\text{TS}_{\text{I}2}$ with an energy barrier of 38.10 kcal/mol, and this process is also endothermic by 36.53 kcal/mol. Thus, these interconversion processes are clearly not feasible, both kinetically and thermodynamically. This implies that methylation of surface silicon, obtained at the early stage of the reaction, remains unaffected by the interconversion process.

Substitution Process. The desired formation of Si–Me on the silicon surface can be achieved through a substitution

process also. The cluster we have considered here is $\text{Si}_9\text{H}_{12}\text{XY}$, where one of the surface silicons is terminated with X and another is terminated with Y. X and Y are chosen in such a way that the termination process is energetically favored and one or both of them are well replaceable through different alkylation processes. In the present study, two methylating reagents are taken into consideration while investigating the substitution process: one is methyl lithium and the other is Grignard reagent (methyl magnesium bromide). Two types of termination processes are adopted here: One is termination with HCl where X is chlorine and Y is hydrogen. In this case, the chlorine of the Si–Cl bond is easily substituted by both methyl magnesium bromide and methyl lithium. Hydrogen is also substitutable through an electrochemical process via a radical mechanism.²⁶ As we are considering a thermal process only, only the Si–Cl substitution process is explored here where we have implemented a concerted $\text{S}_{\text{N}}2$ type mechanism.

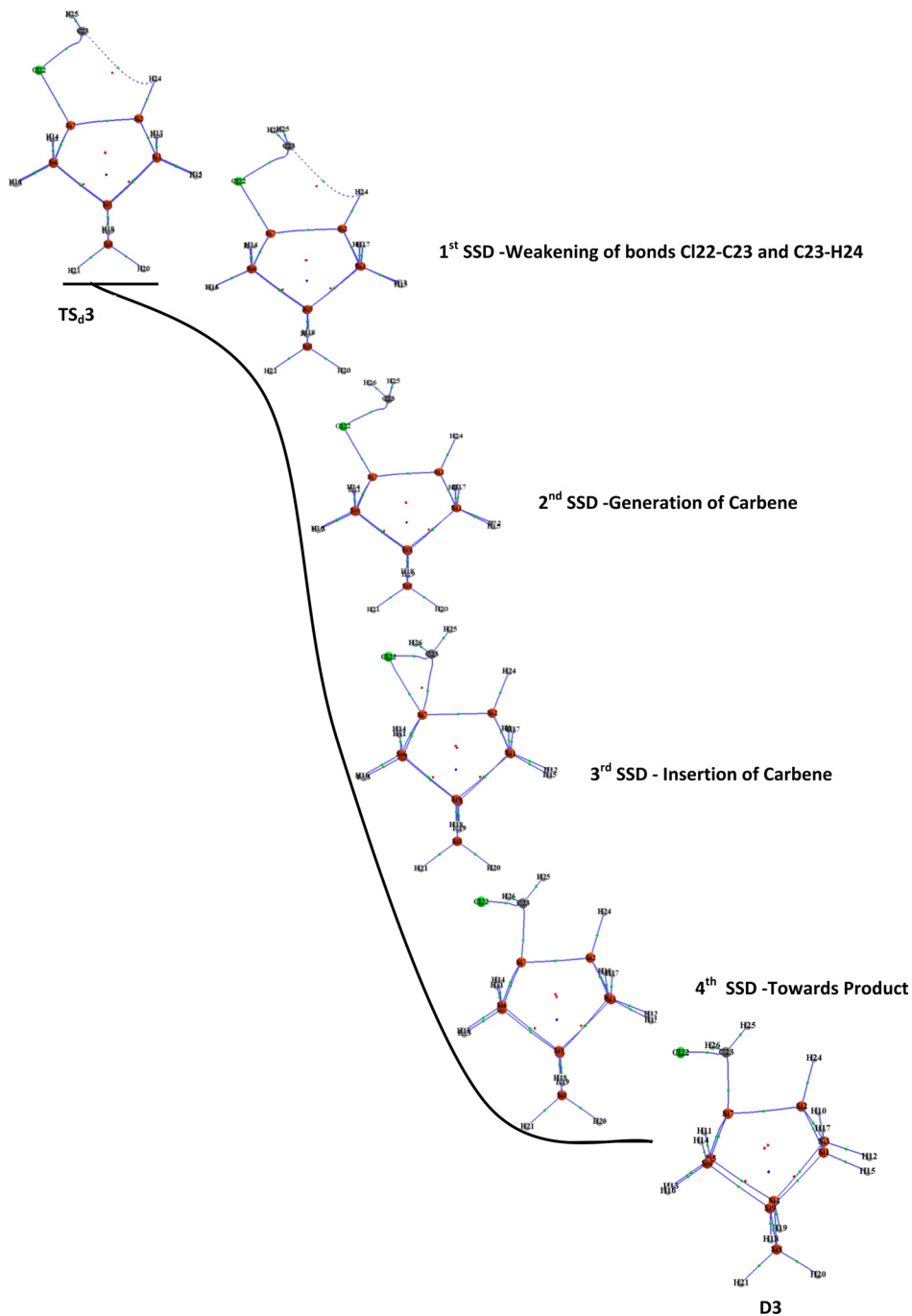


Figure 6. Molecular graph of some structures appearing in the IRC pathway of $\text{TS}_{\text{d}3} \rightarrow \text{D}_3$, to detect in situ carbene formation.

The other termination process is the passivation by Cl_2 where both X and Y are chlorine and both are substitutable using methyl lithium and methyl magnesium bromide.

HCl Termination on Si_9H_{12} . The silicon surface is passivated by HCl to get a Cl-terminated surface in alternative silicon. The process is found to be feasible kinetically as well as thermodynamically. The activation energy for this process is very low, 2.82 kcal/mol, and in addition, the dissociation process is also highly exothermic by 69.21 kcal/mol. The cyclic four-member transition state, TS_{p} , shows that the HCl bond becomes weaker and weak interaction is developed in between silicon–chlorine and silicon–hydrogen and also the Si–Si bond becomes elongated and this leads to the formation of the product P1. In both PES3 and PES4, the passivation pathway of

HCl is shown as an entrance channel for production of D1 by substitution.

Methylation on HCl Terminated Surface. Methylation on the HCl-terminated silicon surface through methyl magnesium bromide and methyl lithium are the types of substitution processes where both methylating agents substitute chlorine with methyl, forming the Si–Me bond and resulting in the formation of D1 (shown in Figure 2), the same product obtained in the CH_4 dissociation process. Both substitution processes pass through well-defined transition states leading to D1. The complete potential energy surface for both substitution processes are shown in PES3 (Figure 7) and PES4 (Figure 8) for methyl lithium and methyl magnesium bromide, respectively.

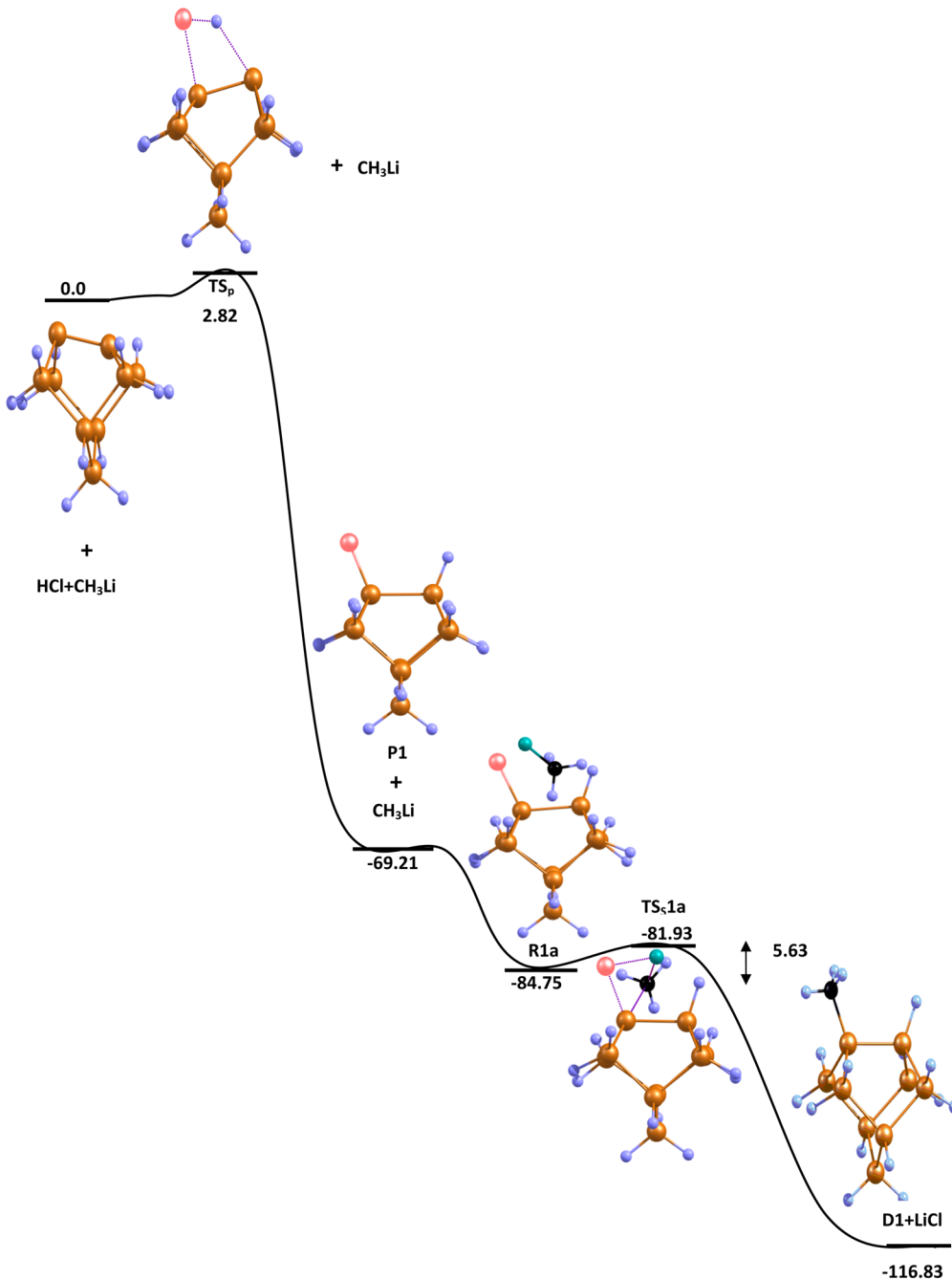


Figure 7. Potential energy surface for substitution reaction with CH₃Li on HCl-passivated Si₉H₁₂ at the M06-2X/6-311+G(2d,p) level (PES3) in kcal/mol.

As PES3 describes, the entrance channel is HCl passivation. After forming P1, CH₃Li forms an adduct with the Si–Si surface, named R1a. Chlorine is then substituted by the methyl group of CH₃Li through TS_s1a to form the monomethylated product D1 along with LiCl. Similarly, in the case of PES4, the HCl passivation process is also shown as the entrance channel. The Si–Si surface forms an adduct with methyl magnesium bromide, designated as R1b, which subsequently forms D1 along with ClMgBr through TS_s1b. Hence, in both of these processes, 50% surface coverage has been achieved.

Carefully looking at the substitution process with methyl lithium, it is observed that the transition state, TS_s1a, is located at an energy level about 2.82 kcal/mol higher than the reactant, and in TS_s1a, Si is weakly bonded with both methyl and

chlorine. The Si–Cl distance is 2.22 Å (Si–Cl single bond length 2.02 Å), and the Si–Me distance is 2.84 Å (Si–C single bond length 1.85 Å). As dictated by the transition vector, formation of the Si–Me bond and rupture of the Si–Cl bond takes place in a concerted manner. The substitution process is found to be highly exothermic by an amount of 42.77 kcal/mol, indicating the process to be thermodynamically favored.

Substitution of chlorine with Grignard reagent is similar to that of methyl lithium. The activation barrier for this process is calculated to be 20.58 kcal/mol, substantially higher than the previous one. The transition state, TS_s1b, holds a Si–Me bond distance of 2.58 Å and a Si–Cl bond distance of 2.44 Å. This substitution process is also found to be highly exothermic, by 30.73 kcal/mol, and thus thermodynamically favored.

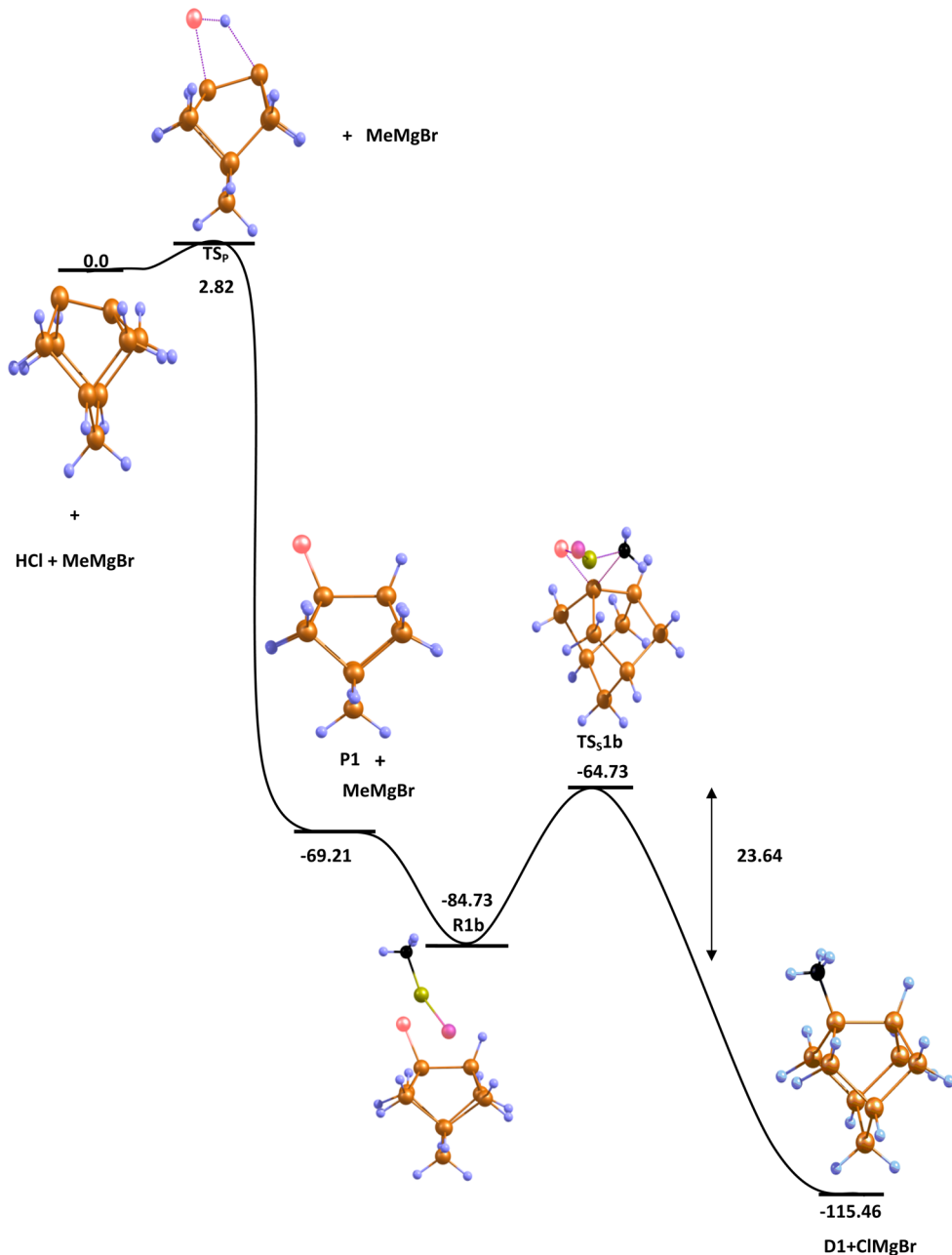


Figure 8. Potential energy surface for the substitution reaction with CH_3MgBr on a HCl -passivated Si_9H_{12} surface at the M06-2X/6-311+G(2d,p) level (PES4) in kcal/mol.

Now, comparing dissociation of CH_4 with these substitution processes, it is evident that the substitution processes are kinetically more favored over dissociation, the differences in activation barriers being about 45.71 kcal/mol for methyl lithium and about 27.95 kcal/mol for Grignard reagent. Therefore, it can be finally concluded that formation of D1 is facilitated by the substitution process involving methyl lithium.

Methylation on Cl_2 Terminated Si_9H_{12} Surface. The Cl_2 -terminated silicon surface can be obtained simply through dissociation of Cl_2 , and here, both chlorines are substitutable using Grignard reagent and methyl lithium. The substitution of first chlorine by methyl renders D2, also obtained previously in the dissociation of CH_3Cl . The first substitution process is referred to as monomethylation forming D2, and the second substitution process is referred to as dimethylation forming S1.

The complete potential energy diagram for the substitution process is demonstrated in PESS (shown in Figure 9) and PES6 (shown in Figure 10) for methyl lithium and methyl magnesium bromide, respectively, on a Cl_2 -passivated silicon surface. Both of the potential energy surfaces follow a similar pattern and give rise to the same methylated products in subsequent steps. The only differences are substituents and energetics. In both cases, substituents form adducts with a Cl_2 -passivated surface named R2a (for methyl lithium) and R2b (for methyl magnesium bromide) and subsequently undergo a substitution mechanism through well-defined transition states, $TSs2a$ and $TSs2b$, respectively, to form a monomethylated product, D2 (with 50% surface coverage), along with byproducts. D2 then forms an adduct with another substituent to form R3a (for methyl lithium) and R3b (for methyl

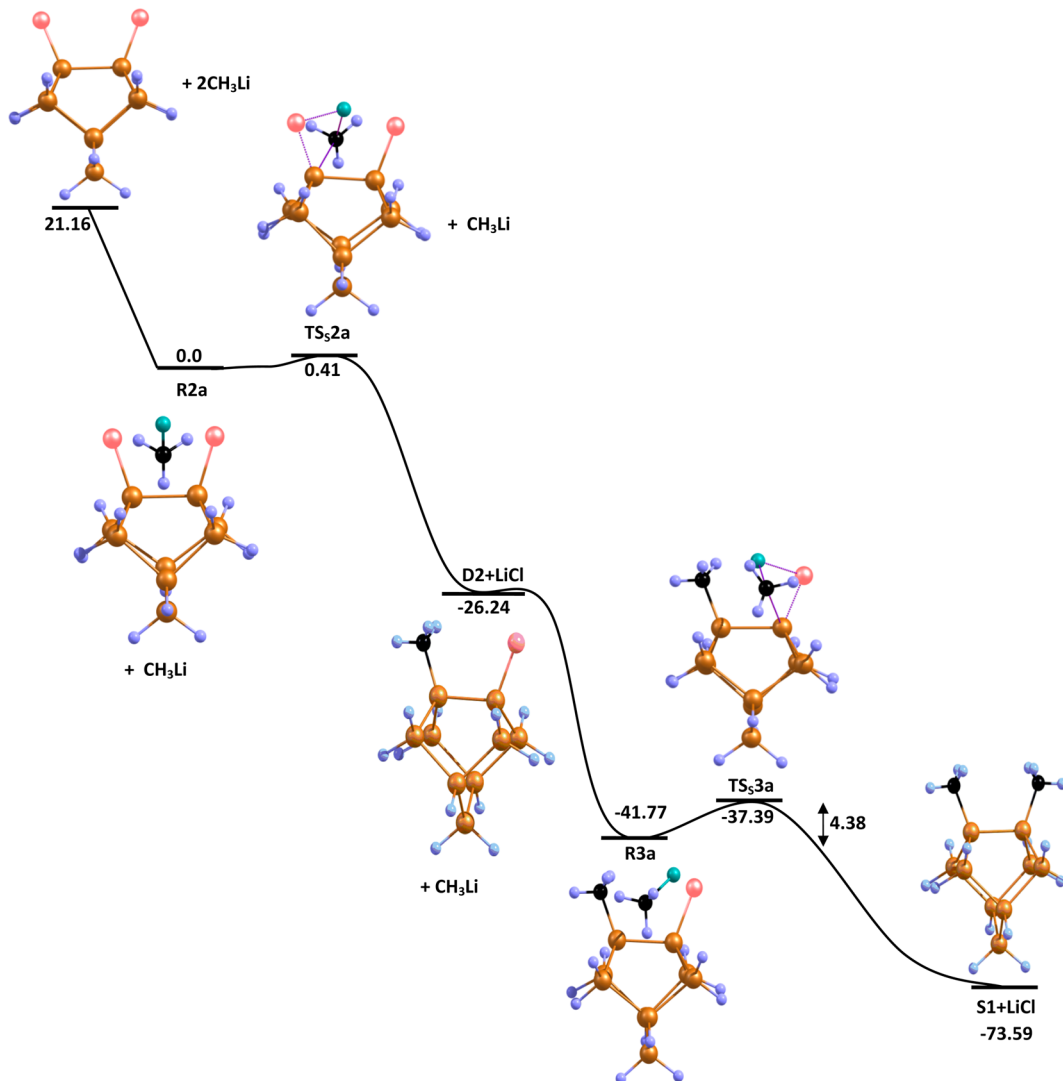


Figure 9. Potential energy surface for the substitution reaction with CH₃Li on Cl₂-passivated Si₉H₁₂ at the M06-2X/6-311+G(2d,p) level (PESS) in kcal/mol.

magnesium bromide), respectively. Following a similar substitution mechanism, a dimethylated product S1 is obtained along with the same byproducts, produced in the first step through the transition states, TS_{s3a} and TS_{s3b}, respectively, giving 100% surface coverage.

The activation barrier associated with the transition state, TS_{s2a}, is found to be only 0.41 kcal/mol, compared to an activation barrier of 17.44 kcal/mol for TS_{s2b}, and this indicates that a monomethylation process with methyl lithium is energetically more favorable than with Grignard reagent. Similarly, as the energetics dictate, dimethylation using methyl lithium is also more favorable than using Grignard reagent. The dimethylation process needs to pass through an activation barrier of 4.38 kcal/mol for methyl lithium and 21.80 kcal/mol for Grignard reagent. From the thermodynamic perspective, methylation using alkyl lithium is also proved to be superior to that of methyl magnesium bromide, the former being more exothermic than the latter. It should be mentioned here that comparing monomethylation with dimethylation, monomethylation is found to be more favorable than dimethylation both kinetically and thermodynamically for both of the substituents.

It should be noted here that the monomethylated product D2 can be produced in two ways: one is through the dissociation of the C–Cl bond of CH₃Cl, and the other is through substitution of the first chlorine in the Cl₂-passivated surface. Subsequently, the dimethylated product (Si₉H₁₂Me₂) can be obtained either through dissociation followed by substitution or through double substitution where only the entrance channels differ. A comparison of the energetics of the two pathways reveals that the double substitution is favored over dissociation followed by substitution, both thermodynamically and kinetically, and this in turn indicates that double substitution through methyl lithium is energetically more viable for the dimethylation process than dissociation followed by substitution. All the activation barriers and enthalpy of reaction values are reported in Table 3 for all the dissociation and substitution processes.

Surface Coverage. Here, we have two types of surface coverage. One is alternate methylation which gives 50% surface coverage (D1 and D2), and the other is continuous methylation which gives 100% surface coverage (S1). In the case of 50% surface coverage, alternate silicon is bonded with hydrogen and chlorine; thus, with respect to device formation the efficiency is

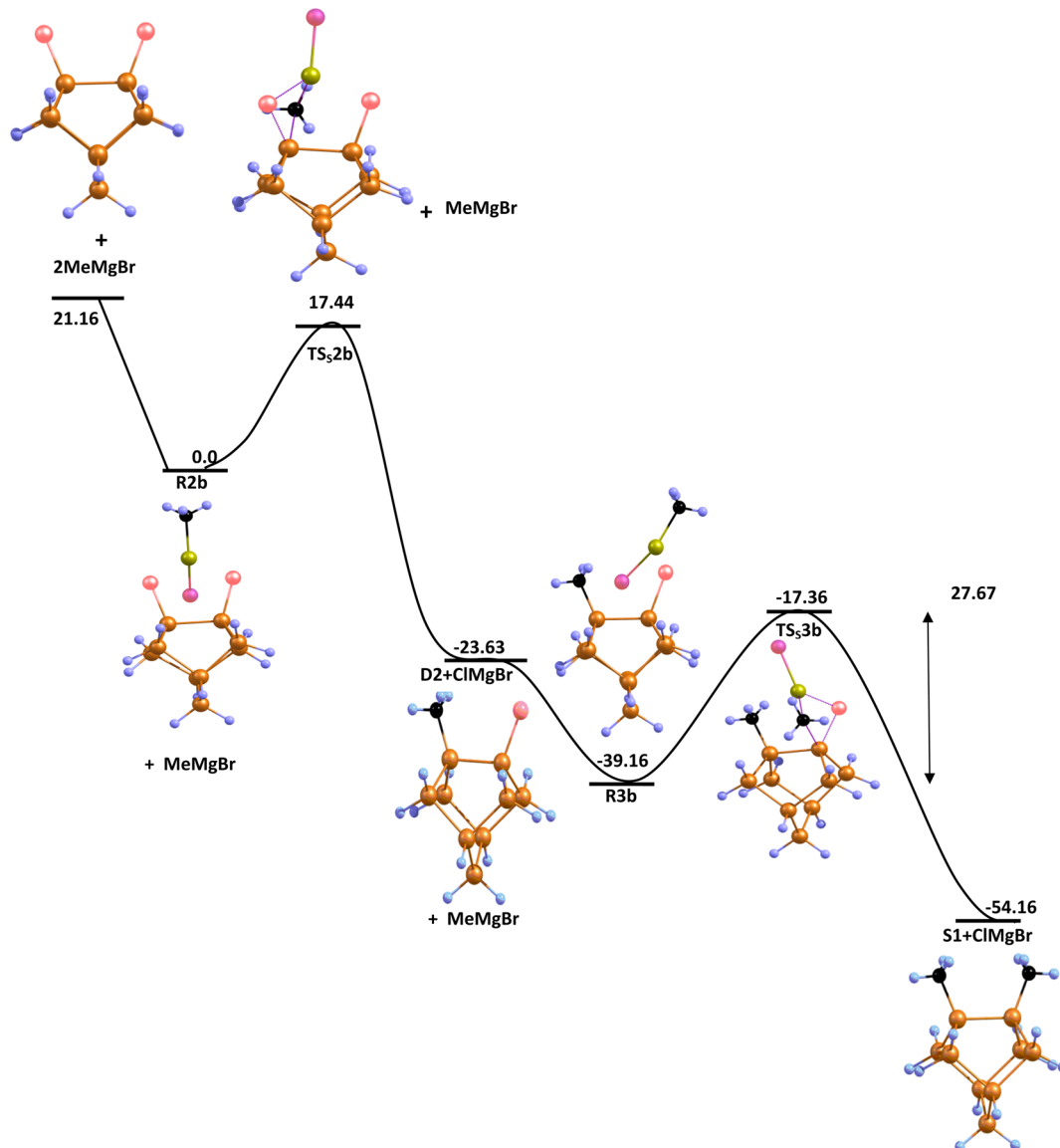


Figure 10. Potential energy surface for substitution reaction with CH_3MgBr on Cl_2 -passivated Si_9H_{12} at the M06-2X/6-311+G(2d,p) level (PES6) in kcal/mol.

Table 3. Activation Energy (E_a) and Enthalpy of Reaction (ΔH_r) of All the Reaction Channels for Schemes 1–4 at the M06-2X/6-311+G(2d,p) Level at 0 °C

reaction	E_a (kcal/mol)	ΔH_r (kcal/mol)
$\text{Si}_9\text{H}_{12} + \text{CH}_4 \rightarrow \text{D}1$	48.53	-46.87
R1a → D1	2.82	-32.08
R1b → D1	20.58	-30.73
A1 → D2	26.48	-77.38
R2a → D2	0.41	-26.24
R2b → D2	17.44	-23.63
A1 → D3	36.23	-40.06
D2 → I1	64.66	34.55
D3 → I2	38.10	36.53
$\text{Si}_9\text{H}_{12} + \text{HCl} \rightarrow \text{P}1$	2.82	-69.21
R3a → S1	4.38	-31.82
R3b → S1	21.80	-30.11

not fully achievable and with respect to inertness the surface is not inert at all, as Si–Cl and to some extent Si–H bonds are

active in air. In the case of D1, alternate silicon is methylated and hydrogenated which indicates there is no scope to increase the surface coverage from 50 to 100%, as it is difficult to replace hydrogen through a concerted substitution process. However, in the case of D2, we initially get 50% coverage where alternate silicon is bonded with chlorine which is further substituted, leading to the formation of S1 as well as 100% surface coverage.

CONCLUSION

In this work, we have systematically examined the possible mechanism of Si–Me bond formation on the silicon surface. Several types of investigations have been carried out to probe into the mechanism. The complete potential energy surface for the dissociation processes of CH_4 and CH_3Cl and the substitution process through methyl lithium and methyl magnesium bromide on HCl^- and Cl_2 -passivated surfaces are thoroughly investigated employing the M062X functional. Two types of methylated products are obtained in this systematic investigation, monomethylated product (D1, D2, and D3) and dimethylated product (S1). D1 is obtained via three path-

ways—dissociation of methane and substitution of chlorine on a HCl-passivated surface through methyl lithium and methyl magnesium bromide. Substitution through methyl lithium is found to be the energetically most favored pathway among the three. Similarly, D₂ is also formed through three pathways—dissociation of CH₃Cl and substitution of chlorine on a Cl₂-passivated surface by methyl lithium and methyl magnesium bromide. Here, also, methyl lithium is observed to be the best reagent. The production of S1 from D2 is the process of substitution where alternative chlorine is substituted to get a dimethylated product with both of the substituents, and in this process, methyl lithium is again proved to be a better substituent than Grignard reagent. Thus, it is well understood from our calculations that methyl lithium is the best methylating agent among the reagents considered here. Analyzing the dissociation process of CH₃Cl only, it is observed that the process of formation of Si-Me (D2) passes through a lower activation barrier than formation of Si-CH₂Cl (D3), and it is also observed that interconversion processes are energetically not favored and thus D2 and D3 rarely follow interconversion steps. Thus, we can conclude D2 is the major product in Scheme 2. With respect to surface coverage, both dissociation followed by substitution and double substitution give 100% surface coverage. As the entrance channel for double substitution is energetically more favored, Scheme 4 with CH₃Li as a substituent is concludingly proved to be the best pathway for methylation with respect to energetics as well as surface coverage among all the schemes adopted here. Our systematic investigation also provides the possible adsorption modes (both physisorption and dissociative adsorption) of CH₃Cl over the silicon surface with all possible potential energy surfaces. The exact physisorption modes are being searched with exact adsorption energies. Interestingly, our work has revealed the possible occurrence of a carbene intermediate during the dissociation of the C-H bond of CH₃Cl over the silicon surface. We expect our work would invite further experimental and theoretical investigations on the methylation process over the silicon surface.

ASSOCIATED CONTENT

Supporting Information

D3-dispersion corrected values and BSSE correction values of all the adsorption modes. The Supporting Information is available free of charge on the ACS Publications website at DOI: 10.1021/acs.jpca.5b01148.

AUTHOR INFORMATION

Corresponding Author

*E-mail: spakd.iacs.res.in.

Notes

The authors declare no competing financial interest.

ACKNOWLEDGMENTS

T.D., K.S., and T.B. are grateful to the Council of Scientific and Industrial Research (CSIR), Government of India, for providing them research fellowships. A.K.D. is grateful to the Department of Science and Technology (DST), Government of India, for a research grant under scheme number: SB/S1/PC-79/2012.

REFERENCES

- Buriak, J. M. Organometallic Chemistry on Silicon and Germanium Surfaces. *Chem. Rev.* **2002**, *102*, 1271–1308.
- Ulman, A. Formation and Structure of Self-Assembled Monolayers. *Chem. Rev.* **1996**, *96*, 1533–1554.
- Maboudian, R. Surface Processes in MEMS Technology. *Surf. Sci. Rep.* **1998**, *30*, 207–269.
- Wayner, D. D. M.; Wolkow, R. A. Organic Modification of Hydrogen Terminated Silicon Surfaces. *J. Chem. Soc., Perkin Trans. 2* **2002**, *1*, 23–34.
- Linford, M. R.; Chidsey, C. E. D. Alkyl Monolayers Covalently Bonded to Silicon Surfaces. *J. Am. Chem. Soc.* **1993**, *115*, 12631–12632.
- Ulman, A. *An Introduction to Ultrathin Organic Films from Langmuir-Blodgett to Self-Assembly*; Academic Press: New York, 1991.
- Faber, E. J.; de Smet, L. C. P. M.; Olthuis, W.; Zuilhof, H.; Sudhölter, E. J. R.; Bergveld, P.; van den Berg, A. Si-C Linked Organic Monolayers on Crystalline Silicon Surfaces as Alternative Gate Insulators. *ChemPhysChem* **2005**, *6*, 2153–2166.
- Liu, Y.-J.; Yu, H.-Z. Alkyl Monolayer Passivated Metal-Semiconductor Diodes: Comparison with Native Silicon Oxide. *ChemPhysChem* **2003**, *4*, 335–342.
- Scheibal, Z. R.; Xu, W.; Audiffred, J. F.; Henry, J. E.; Flake, J. C. Protein Immobilization onto Silicon Nanowires via Electrografting of Hexynoic Acid. *Electrochem. Solid-State Lett.* **2008**, *11*, K81–K84.
- Kilian, K. A.; Böcking, T.; Gaus, K.; Gal, M.; Gooding, J. J. Si-C linked Oligo(Ethylene Glycol) Layers in Silicon-Based Photonic Crystals: Optimization for Implantable Optical Materials. *Biomaterials* **2007**, *28*, 3055–3062.
- (11) Varadan, V. K.; Varadan, V. V. *Smart Mater. Struct.* **2000**, *9* (6), 953–972.
- Zhu, X. Y.; Houston, J. E. Molecular Lubricants for Silicon-Based Microelectromechanical Systems (MEMS): A Novel Assembly Strategy. *Tribol. Lett.* **1999**, *7*, 87–90.
- Blackmore, J. S. *Semiconductor Statistics*; Dover Publications: New York, 1987.
- Gstrein, F.; Michalak, D. J.; Royea, W. J.; Lewis, N. S. Effects of Interfacial Energetics on the Effective Surface Recombination Velocity of Si/Liquid Contacts. *J. Phys. Chem. B* **2002**, *106*, 2950–2961.
- Rivillon Amy, S.; Michalak, D. J.; Chabal, Y. J.; Wielunski, L.; Hurley, P. T.; Lewis, N. S. Investigation of the Reactions during Alkylation of Chlorine-Terminated Silicon (111) Surfaces. *J. Phys. Chem. C* **2007**, *111*, 13053–13061.
- Nemanick, E. J.; Hurley, P. T.; Brunschwig, B. S.; Lewis, N. S. Chemical and Electrical Passivation of Silicon (111) Surfaces through Functionalization with Sterically Hindered Alkyl Groups. *J. Phys. Chem. B* **2006**, *110*, 14800–14808.
- Brook, M. A. *Silicon in Organic, Organometallic and Polymer Chemistry*; Wiley: New York, 2000.
- Schmeltzer, J. M.; Porter, L. A.; Stewart, M. P.; Buriak, J. M. Hydride Abstraction Initiated Hydrosilylation of Terminal Alkenes and Alkynes on Porous Silicon. *Langmuir* **2002**, *18*, 2971–2974.
- Teyssot, A.; Fidélis, A.; Fellah, S.; Ozanam, F.; Chazalviel, J. N. Anodic Grafting of Organic Groups on the Silicon Surface. *Electrochim. Acta* **2002**, *47*, 2565–2571.
- Faucheur, A.; Gouget-Laemmel, A. C.; Henry de Villeneuve, C.; Boukherroub, R.; Ozanam, F.; Allongue, P.; Chazalviel, J.-N. Well-Defined Carboxyl-Terminated Alkyl Monolayers Grafted onto H-Si(111): Packing Density from a Combined AFM and Quantitative IR Study. *Langmuir* **2005**, *22*, 153–162.
- Koiry, S. P.; Aswal, D. K.; Saxena, V.; Padma, N.; Chauhan, A. K.; Joshi, N.; Gupta, S. K.; Yakhmi, J. V.; Guerin, D.; Vuillaume, D. Electrochemical Grafting of Octyltrichlorosilane Monolayer on Si. *Appl. Phys. Lett.* **2007**, *90*, 113118 (1)–113118 (3).
- Lee, J. Y.; Kim, S. Adsorption Mechanism of CH₃Cl on Si(100)-2 × 1. *Surf. Sci.* **2001**, *482*–485, Part 1 (0), 196–200.
- Romero, A. H.; Sbraccia, C.; Silvestrelli, P. L.; Ancilotto, F. Adsorption of Methylchloride on Si(100) from First Principles. *J. Chem. Phys.* **2003**, *119*, 1085.

- (24) Qu, Y.-Q.; Li, J.; Han, K.-L. Dissociative Adsorption of Methylsilane on the Si(100)-2 × 1 Surface. *J. Phys. Chem. B* **2004**, *108*, 15103–15109.
- (25) Rivillon Amy, S.; Michalak, D. J.; Chabal, Y. J.; Wielunski, L.; Hurley, P. T.; Lewis, N. S. Investigation of the Reactions During Alkylation of Chlorine-Terminated Silicon (111) Surfaces. *J. Phys. Chem. C* **2007**, *111*, 13053–13061.
- (26) Vegunta, S. S. S.; Ngunjiri, J. N.; Flake, J. C. Electrochemical and Thermal Grafting of Alkyl Grignard Reagents onto (100) Silicon Surfaces. *Langmuir* **2009**, *25*, 12750–12756.
- (27) Herrera, M. U.; Ichii, T.; Murase, K.; Sugimura, H. Photochemical Grafting of Methyl Groups on a Si(111) Surface Using a Grignard Reagent. *J. Colloid Interface Sci.* **2013**, *411*, 145–151.
- (28) Song, J. H.; Sailor, M. J. Functionalization of Nanocrystalline Porous Silicon Surfaces with Aryllithium Reagents: Formation of Silicon–Carbon Bonds by Cleavage of Silicon–Silicon Bonds. *J. Am. Chem. Soc.* **1998**, *120*, 2376–2381.
- (29) Addamiano, A.; Klein, P. H. Chemically-Formed Buffer Layers for Growth of Cubic Silicon Carbide on Silicon Single Crystals. *J. Cryst. Growth* **1984**, *70*, 291–294.
- (30) Shibahara, K.; Nishino, S.; Matsunami, H. Surface Morphology of Cubic SiC(100) Grown on Si(100) by Chemical Vapor Deposition. *J. Cryst. Growth* **1986**, *78*, 538–544.
- (31) De Smet, L. C. P. M.; Zuilhof, H.; Sudhölter, E. J. R.; Lie, L. H.; Houlton, A.; Horrocks, B. R. Mechanism of the Hydrosilylation Reaction of Alkenes at Porous Silicon: Experimental and Computational Deuterium Labeling Studies. *J. Phys. Chem. B* **2005**, *109*, 12020–12031.
- (32) Sieval, A. B.; Opitz, R.; Maas, H. P. A.; Schoeman, M. G.; Meijer, G.; Vergeldt, F. J.; Zuilhof, H.; Sudhölter, E. J. R. Monolayers of 1-Alkynes on the H-Terminated Si(100) Surface. *Langmuir* **2000**, *16*, 10359–10368.
- (33) Konecny, R.; Doren, D. J. Adsorption of BH₃ on Si(100)-2 × 1. *J. Phys. Chem. B* **1997**, *101*, 10983–10985.
- (34) Bacalzo, F. T.; Musaev, D. G.; Lin, M. C. Theoretical Studies of CO Adsorption on Si(100)-2 × 1 Surface. *J. Phys. Chem. B* **1998**, *102*, 2221–2225.
- (35) Bacalzo-Gladden, F.; Lu, X.; Lin, M. C. Adsorption, Isomerization, and Decomposition of HCN on Si(100)-2 × 1: A Computational Study with a Double-Dimer Cluster Model. *J. Phys. Chem. B* **2001**, *105*, 4368–4373.
- (36) Zhang, L.; Carman, A. J.; Casey, S. M. Adsorption and Thermal Decomposition Chemistry of 1-Propanol and Other Primary Alcohols on the Si(100) Surface. *J. Phys. Chem. B* **2003**, *107*, 8424–8432.
- (37) Ferguson, G. A.; Das, Ü.; Raghavachari, K. Interaction of Lewis Acids with Si(100)-2 × 1 and Ge(100)-2 × 1 Surfaces. *J. Phys. Chem. C* **2009**, *113*, 10146–10150.
- (38) Sniatycksi, R.; Janesko, B. G.; El-Mellouhi, F.; Brothers, E. N. Application of Screened Hybrid Density Functional Theory to Ammonia Decomposition on Silicon. *J. Phys. Chem. C* **2012**, *116*, 26396–26404.
- (39) Barriocanal, J. A.; Doren, D. J. Reactions of Nitromethane on Si(100): First-Principles Predictions. *J. Phys. Chem. B* **2000**, *104*, 12269–12274.
- (40) Lu, X.; Xu, X.; Wang, N.; Zhang, Q.; Lin, M. C. Chemisorption and Decomposition of Thiophene and Furan on the Si(100)-2 × 1 Surface: A Quantum Chemical Study. *J. Phys. Chem. B* **2001**, *105*, 10069–10075.
- (41) Zhu, Z.; Srivastava, A.; Osgood, R. M. Reactions of Organosulfur Compounds with Si(100). *J. Phys. Chem. B* **2003**, *107*, 13939–13948.
- (42) Wang, G. T.; Mui, C.; Musgrave, C. B.; Bent, S. F. Effect of a Methyl-Protecting Group on the Adsorption of Pyrrolidine on Si(100)-2 × 1. *J. Phys. Chem. B* **2001**, *105*, 3295–3299.
- (43) Widjaja, Y.; Han, J. H.; Musgrave, C. B. Quantum Chemical Study of Zirconium Oxide Deposition on the Si(100)-(2 × 1) Surface. *J. Phys. Chem. B* **2003**, *107*, 9319–9324.
- (44) Liu, Y.; Wang, Z. Addition Reaction of Nitrones on the Reconstructed Si(100)-2 × 1 Surface. *J. Phys. Chem. C* **2007**, *111*, 4673–4677.
- (45) Halls, M. D.; Raghavachari, K. Atomic Layer Deposition Growth Reactions of Al₂O₃ on Si(100)-2 × 1. *J. Phys. Chem. B* **2004**, *108*, 4058–4062.
- (46) Kato, T.; Kang, S.-Y.; Xu, X.; Yamabe, T. Possible Dissociative Adsorption of CH₃OH and CH₃NH₂ on Si(100)-2 × 1 Surface. *J. Phys. Chem. B* **2001**, *105*, 10340–10347.
- (47) Ardalan, P.; Dupont, G.; Musgrave, C. B. Reactions of Amino Acids on the Si(100)-2 × 1 Surface. *J. Phys. Chem. C* **2011**, *115*, 7477–7486.
- (48) Ferguson, A. G.; Ramabhadran, R. O.; Than, C. T. L.; Paradise, R. K.; Raghavachari, K. Reactions of Atomic Hydrogen with the Hydroxide- and Amine- Functionalized Si(100)-2 × 1 Surfaces: Accurate Modeling of Hydrogen Abstraction Reactions Using Density Functional Theory. *J. Phys. Chem. C* **2014**, *118*, 8379–8386.
- (49) Raghavachari, K.; Halls, M. D. Quantum Chemical Studies of Semiconductor Surface Chemistry Using Cluster Models. *Mol. Phys.* **2004**, *102*, 381–393.
- (50) Zhao, Y.; Truhlar, D. The M06 Suite of Density Functionals for Main Group Thermochemistry, Thermochemical Kinetics, Non-covalent Interactions, Excited States, and Transition Elements: Two New Functionals and Systematic Testing of Four M06-Class Functionals and 12 Other Functionals. *Theor. Chem. Acc.* **2008**, *120*, 215–241.
- (51) Gonzalez, C.; Schlegel, H. B. An Improved Algorithm for Reaction Path Following. *J. Chem. Phys.* **1989**, *90*, 2154–2161.
- (52) Gonzalez, C.; Schlegel, H. B. Reaction Path Following in Mass-Weighted Internal Coordinates. *J. Phys. Chem.* **1990**, *94*, 5523–5527.
- (53) Grimme, S.; Antony, J.; Ehlrich, S.; Krieg, H. A. A Consistent and Accurate Ab Initio Parameterization of Density Functional Correction (DFT-D) for the 94 Elements H–Pu. *J. Chem. Phys.* **2010**, *132*, 154104.
- (54) Grimme, S.; Ehlrich, S.; Goerigk, L. Effect of the Damping Function in Dispersion Corrected Density Functional Theory. *J. Comput. Chem.* **2011**, *7*, 1456–1465.
- (55) Boys, S. F.; Bernardi, F. Calculation of Small Molecular Interactions by Differences of Separate Total Energies - Some Procedures with Reduced Errors. *Mol. Phys.* **1970**, *19*, 553.
- (56) Simon, S.; Duran, M.; Dannenberg, J. J. How Does Basis Set Superposition Error Change the Potential Surfaces for Hydrogen Bonded Dimers? *J. Chem. Phys.* **1996**, *105*, 11024–11031.
- (57) Goerigk, L.; Grimme, S. A. Thorough Benchmark of Density Functional Methods for General Main Group Thermochemistry, Kinetics and Noncovalent Interactions. *Phys. Chem. Chem. Phys.* **2011**, *13*, 6670–6688.
- (58) Frisch, M. J.; Trucks, G. W.; Schlegel, H. B.; Scuseria, G. E.; Robb, M. A.; Cheeseman, J. R.; Scalmani, G.; Barone, V.; Mennucci, B.; Petersson, G. A.; Nakatsuji, H.; Caricato, M.; Li, X.; Hratchian, H. P.; Izmaylov, A. F.; Bloino, J.; Zheng, G.; Sonnenberg, J. L.; Hada, M.; Ehara, M.; Toyota, K.; Fukuda, R.; Hasegawa, J.; Ishida, M.; Nakajima, T.; Honda, Y.; Kitao, O.; Nakai, H.; Vreven, T.; Montgomery, J. A.; Peralta, J. E.; Ogliaro, F.; Bearpark, M.; Heyd, J. J.; Brothers, E.; Kudin, K. N.; Staroverov, V. N.; Kobayashi, R.; Normand, J.; Raghavachari, K.; Rendell, A.; Burant, J. C.; Iyengar, S. S.; Tomasi, J.; Cossi, M.; Rega, N.; Millam, J. M.; Klene, M.; Knox, J. E.; Cross, J. B.; Bakken, V.; Adamo, C.; Jaramillo, J.; Gomperts, R.; Stratmann, R. E.; Yazayev, O.; Austin, A. J.; Cammi, R.; Pomelli, C.; Ochterski, J. W.; Martin, R. L.; Morokuma, K.; Zakrzewski, V. G.; Voth, G. A.; Salvador, P.; Dannenberg, J. J.; Dapprich, S.; Daniels, A. D.; Farkas, Foresman, J. B.; Ortiz, J. V.; Cioslowski, J.; Fox, D. J. *Gaussian 09*, revision B.01; Gaussian, Inc.: Wallingford, CT, 2009.
- (59) Keith, T. A. *AIMALL*, version 11.08.23; TK Gristmill Software: Overland Park, KS, 2011.
- (60) Bader, R. F. W. *Atoms in Molecules - A Quantum Theory*; Oxford University Press: Oxford, U.K., 1990.